# Cold-Drawn Material As Model Material for the Environmental Stress Cracking (ESC) Phenomenon in Polyethylene. A Raman Spectroscopy Study of Molecular Stress Induced by Macroscopic Strain in Drawn Polyethylenes and Their Relation to Environmental Stress Cracking

**José M. Lagarón,[†] N. Michael Dixon,[‡] Don L. Gerrard,[‡] Warren Reed,[‡] and Bert J. Kip*,[†]**

*DSM Research, P.O. Box 18, 6160 MD Geleen, The Netherlands, and BP Chemicals, Chertsey Road, Sunbury-on-Thames TW16 7LN, U.K.*

*Received December 2, 1997; Revised Manuscript Received March 25, 1998*

ABSTRACT: Raman spectroscopy was used to study strain-induced molecular stress in cold-drawn polyethylenes, which were being used as a model system for fibrils present in the crazes formed during environmental stress crack resistance (ESCR) tests. The molecular stress was measured at 240 K in order to minimize relaxation phenomena. Molecular stress was related to macroscopic strain and, by correcting for differences in *E*-moduli, to true stress. In this paper, the measured molecular stress is related to ESCR values and sample characteristics. It was observed that good ESCR materials showed a lower molecular stress than worse ESCR materials at the same macroscopic strain level. It was also observed that the molecular weight has a major effect on the observed molecular stress per macroscopic strain (molecular stress per macroscopic strain decreases with increasing $M_w$), whereas the effect of chain branching is smaller (molecular stress per macroscopic strain decreases with chain branching).

## Introduction

Environmental stress cracking (ESC) is a slow crack growth process which results from a continuously applied small load in the neighborhood of room temperature and in the presence of an aggressive environment. This mode of failure is characterized by the presence of macroscopic "cracks" and a fibrillar structure of the craze, formed ahead of the crack. The ESC process is particularly relevant to polyethylene (PE) properties and the resulting material lifetimes. Environmental stress crack resistance (ESCR) is of crucial importance in PE applications such as pipes, containers, bottles, and geomembranes. In practice, the process is relatively slow but is still important regarding long-time behavior. Laboratory tests that accelerate the process using detergents and higher loads and temperatures have been developed. The most commonly used methods are the Bell Telephone test (BTT),[1] the bottle stress crack test (BSC),[2,3] and tests making use of notched samples.[4]

All of the laboratory tests take from 1 h to more than 1000 h, and consequently, a more rapid test,[5,6] ca. 3 h, which involves measuring the creep rate of cold-drawn material, was recently developed. The creep rate deceleration factor (CRDF) of material cold-drawn up to the natural draw ratio (NDR), defined as the draw ratio at which the full gauge length of the dumbbell is necked, was found to correlate with the BSC test failure time.[6] These results suggest that the creep process happening in the craze fibrils controls crack formation and/or propagation and that cold-drawn material could be a useful starting material for studying the ESC phenomenon. However, it is surprising that the ranking of the high-temperature ESCR tests can be predicted accurately from creep tests performed at room temperature on cold-drawn samples, since the structure of the crystalline phase and the associated relaxation processes are temperature dependent.[7]

Several molecular mechanisms for ESC have been proposed over the past few years. Lustiger et al.[8,9] have proposed "interlamellar failure" as the controlling mechanism of ESC, with the concentration of tie molecules as a factor in ESCR. The environment is thought to lubricate the "interlamellar failure". Tie molecules are defined as molecules that pass repeatedly through lamellae and amorphous regions in the polymer. Materials with the higher molecular weight and the comonomer content located in the higher molecular weight (bimodal polyethylenes) were shown to give the largest concentration of tie molecules. Brown et al.[10] concluded the mechanism of slow crack growth involves the disentanglement of the molecules through the crystalline regions and that the number of tie molecules and the strength of the crystals that anchor them are considered the controlling factors.

Infrared and particularly Raman spectroscopy have been used to obtain molecular information from strained polymers[11−13] since changes in bond lengths and bond angles induced by the applied stress can change the vibrational frequencies of specific bands.[14−16] Molecular deformation in ultraoriented high molecular weight polyethylene have been extensively studied.[17−20] From these studies the relationship between molecular strain and the shift of vibrational bands has been established. For polyethylene, the backbone C−C stretching modes at 1060 $cm^{-1}$ (asymmetric stretching) and 1130 $cm^{-1}$ (symmetric C−C stretching) are particularly sensitive to molecular strain and were found to shift by 14 and 8.7 $cm^{-1}$/% molecular strain, respectively.

As a consequence of the above, it was thought that a Raman spectroscopic study of the deformation behavior of cold-drawn specimens might provide both a quick ESCR measurement technique as well as more detailed information on the molecular mechanisms involved in

[†] DSM Research.
[‡] BPChemicals.

S0024-9297(97)01760-9 CCC: $15.00 
Published on Web 08/08/1998

**Table 1. Some Material Properties of the Seven HDPE Samples Studied**

| sample | density (kg/m$^3$) | $M_w$ ($\times 10^3$) | $M_w/M_n$ | SCB/1000C[a] | $E$[b] (GPa) | NDR | PE type |
|---|---|---|---|---|---|---|---|
| A | 960 | 134 | 7.4 | 0 | 14.7 | 10.4 | homopolymer |
| B | 954 | 385 | 8.0 | 0 | 5.1 | 7.0 | homopolymer |
| C | 958 | 200 | 18.2 | 0.3 (E) | 9.8 | 8.7 | unimodal copolymer |
| D | 950 | 346 | 15.0 | 0.17 (E) | 5.3 | 6.2 | unimodal copolymer |
| E | 945 | 300 | 13 | 1.2 (E) | 4.2 | 5.6 | unimodal copolymer |
| F | 931 | 1570 | 5.8 | 0 | 1.2 | 3.5 | homopolymer |
| G | 949 | 405 | 31.1 | 2.0 (B)<br>0.3 (E) | 7.2 | 6.0 | bimodal copolymer |

[a] Short chain branches (SCB), (E) ethyl branches, (B) butyl branches. [b] Initial moduli (between 0 and 1% strain) of the cold-drawn material at 240 K.

stress cracking. The rationale for this is the following. Despite the particular molecular mechanism's leading to stress cracking, it is the different molecular architecture of the materials that is the key fact behind their different responses to ESC. This conclusion is implicit within most models proposed in the literature dealing with ESC mechanisms. With Raman a response from the molecular level (all-trans segments strain) is probed. The observed band shifts probe the stress in all-trans chain segments, those are in principle within crystallites. Straining of the samples will result in tightening of the tie molecules, which will transfer the stress to the crystals. Therefore, the stress in the all-trans sequences present in the crystalline domains might correlate with the stress in the chains connecting the crystalline regions and consequently might correlate with ESC behavior.

In the present study, seven polyethylenes with different molecular characteristics were studied with both conventional ESCR techniques and Raman spectroscopy. In this study, the Raman bands were collected over 1000−1600 cm$^{-1}$. This range is usually divided into three areas:[21,22] (1) C−C stretching between 1000 and 1200 cm$^{-1}$, sensitive to molecular orientation, stress, and conformation; (2) $-CH_2-$ twisting vibrations around 1295 cm$^{-1}$, which can be used as an internal standard; and (3) $-CH_2-$ bending modes between 1400 and 1470 cm$^{-1}$, sensitive to chain packing.

In the present study only the two first ranges were examined in detail. To separate loading of the molecules on the molecular scale and relaxation phenomena, the experiments were performed at 240 K. The relaxation phenomena, i.e., mainly the $\alpha$ and likely the $\beta$ relaxation processes, are thought to be highly suppressed at 240 K[18,23] with respect to the spectral accumulation time (10−100 s). Additional experiments were done at 210 K to further study the relaxation.

## Materials and Methods

**Samples.** The samples studied were three linear PE homopolymers and four high-density PE copolymers. Some sample properties are shown in Table 1.

The cold-drawn samples were obtained by pressing sheets 500 $\mu$m thick between aluminum foils from pellet material in four steps; 5 min at 20 kN at 463 K, 5 min at 200 kN at 463 K, under 200 kN cooling to 308 K and without pressure down to room temperature. From these sheets, dumbbell samples were die-stamped with a gauge length of 20 ± 0.5 mm and a width of 4 ± 0.1 mm (model ISO 527-2:1993 type 5A). The dumbbells were conditioned in boiling water for 30 min to remove any residual stresses built up in the sample preparation procedure.

The cold-drawing was carried out on a Zwick 1455 stretching device with a constant rate of 10 mm/min until the full gauge length of the dumbbell was necked. The natural draw ratio (NDR) is defined by this situation. The NDR was measured with an optical extensometer. The $E$-moduli were estimated from data extracted from tensile tests with the Zwick 1445 stretching device at 240 K. The sample chamber temperature control is ±1 K. This tensile test was performed by straining up to 1% strain at the rate of 10 mm/min of a drawn segment, cut from the cold-drawn sample gauche section, of typically 75 mm length. The $E$-moduli were calculated from the tangent line over the 0−1% strain and are averaged over four experiments.

**Standard ESCR Tests.** The bottle stress crack (BSC) test was performed on cylindrical shaped bottles with a volume of 110 mL and a circular inset panel on one side. The bottles were filled with detergent solution (Igepal:CO-630), screwed into a Tufnol cap, pressurized (0.35 bar), and placed in a water bath (temperature 333 ± 0.5 K). Failure was detected by a decrease to a preset value in the electrical resistance between electrodes placed inside the bottle and the water bath.

The Bell Telephone test (BTT) was performed on a die-stamped "U" bent sample following ref 1. The deformed specimen was transferred to a metal-channeled sample holder and exposed to neat nonylphenylpoly(oxyethylene) (Igepal: CO-630) at 323 K. Ten samples were tested for each polymer. Failure is defined as the appearance of any crack visible to the naked eye.

An ESCR notch test is performed at DSM using a sample of 63 × 12.7 mm with a thickness of 1.0 mm. A double-sided notch (0.25 × 1.95 mm, notch angle 35°) was pressed in the middle of the sample to concentrate the stress during the test. The sample was placed in a detergent solution (Humifen SF-90) at 348 K under a constant load of 3 N/mm$^2$. The time until complete failure of 5−10 samples was recorded.

**Raman Measurements.** The Raman equipment used consisted of a Jobin Yvon (J-Y) U1000 grating spectrometer (600 grooves/mm gratings), as described in ref 24, using 20 mW (at sample) 514 nm excitation, a ×50 short working distance, and a ×50 long working distance objective. Typical integration times were 80−120 s.

An in-house-made bidirectional stretching device was attached to the DSM Raman microscope, to deform uniaxially the cold-drawn specimens at 240 K. The bidirectional character of the stretching device enables one to record Raman spectra at approximately the same sampling point during the stepwise straining of the sample. The stretching device temperature can be controlled with an accuracy of ±1 K by flowing nitrogen gas into the sealed sample chamber. Sample strain was applied by hand and monitored with an extensiometer device with an accuracy of ±0.01 mm. No stress measurement was present. Raman spectra were recorded during the in-situ deformation of the sample.

An indication of the molecular orientation of the various samples was obtained by calculating the 1130/1060 cm$^{-1}$ band area ratio in the polarized Raman spectra, i.e., in the parallel−parallel spectra. ($^{\parallel}I_{\parallel}$, polarization of the incoming laser beam and of scattered light parallel to sample deformation direction). Two other polarization conditions were used in this study. Parallel ($^{\parallel}I$) polarization was obtained using only the incoming laser beam polarized parallel to the sample deformation direction and no polarization analyzer and circular ($^{\circlearrowright}I$) polarization was obtained using a $\lambda/4$ plate between the laser beam

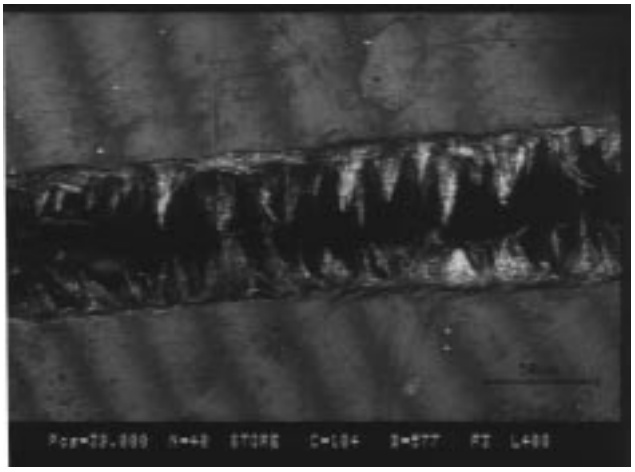

**Figure 1.** SEM image of fibrils in the crack of a BSC failed sample (sample A).

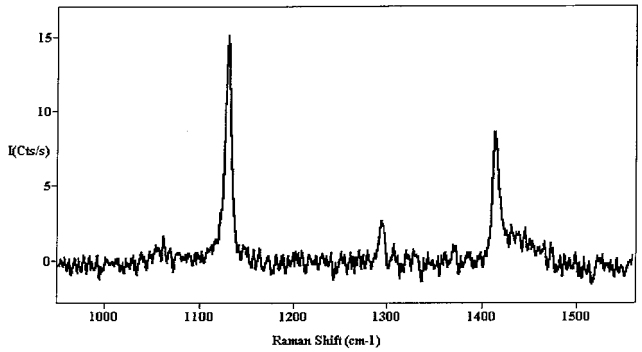


**Figure 2.** Micro-Raman spectrum taken in fibrils of Figure 1 under parallel−parallel ($^{\parallel}I_{\parallel}$) polarization conditions. The spectrum was recorded with the Jovin Yvon system equipped with 600 g/mm gratings.[24] A 50× short working distance objective and 300 $\mu$m pinhole were used as the setup of the microscope.

and the sample, which results in circularly polarized excitation, and again no polarization analyzer.

**Spectral Data Processing.** The spectra were processed with the fitting routine in GRAMS Research 2000 software package (Galactic). Voigt line shapes (convolution of Lorentzian and Gaussian band shapes) and linear baselines were used. To measure band shifts and areas of the 1060, 1130, and 1295 cm$^{-1}$ Raman bands at 240 K, the 1000−1350 cm$^{-1}$ spectral range was fitted using single components for each band. The accuracy of the obtained band positions was estimated to be ± 0.15 cm$^{-1}$.

## Results and Discussions

**ESCR Failure.** The fibrillar structure of the craze, formed ahead of the crack in the ESCR test, is shown in Figure 1 (sample A). A micro-Raman spectrum taken from these fibrils (parallel−parallel polarization conditions ($^{\parallel}I_{\parallel}$)) is shown in Figure 2. This region is sensitive to the molecular arrangement, and the fibril spectrum shows a relatively high molecular orientation of the fibrillar material in the direction perpendicular to crack development.

**Standard ESCR Tests.** The ESCR times of the materials tested using the notch test, the BTT, and the BSC test, are shown in Table 2. Clearly, the ESCR of the high molecular weight materials (B, D, E, F, and G) are higher than those of the materials with relatively low molecular weight (A and C). The presence of branches also increases the ESCR. Note how the bimodal architecture of sample G, with a large $M_w/M_n$ (polydispersity index) and a relatively high density, results in a very good ESCR. The bimodal materials show a good stiffness to toughness balance with a superior ESCR. The ultrahigh molecular weight material (sample F) has also a superior ESCR. This behavior is likely caused by the presence of extremely long molecules, which produce a very entangled molecular network.

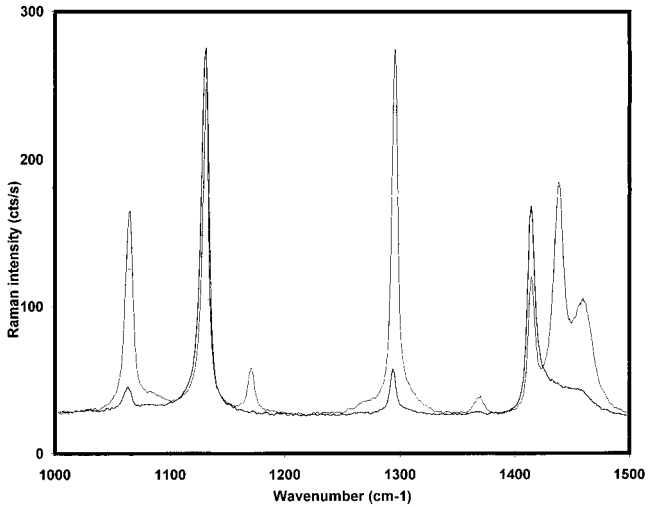


**Figure 3.** Micro-Raman spectra taken in undeformed and cold-drawn (thicker) specimen of sample A under ($^{\parallel}I_{\parallel}$) polarization conditions. The spectra were recorded with the J-Y parallel−parallel equipment. A 50× short working distance objective and ca. 500 $\mu$m pinhole were used as the setup of the microscope.

**Table 2. Notch Test, BTT, and BSC Test Values for Samples A−G (NA = Not Available)**

| | notch test (h) 348 K | BTT (h) 323 K | BSC (h) 333 K |
|---|---|---|---|
| A | 5 | 11 | 1 |
| B | 72 | 200 | 100 |
| C | 10 | 130 | 11 |
| D | 235 | >1000 | 200 |
| E | 651 | >1000 | 530 |
| F | NA | NA | >1000 |
| G | NA | NA | >1000 |

**Molecular Orientation before and after Cold-Drawing.** Samples A (low ESCR) and E (high ESCR) were studied at room temperature (RT) before and after cold drawing, respectively ($^{\parallel}I_{\parallel}$). The Raman spectra show that the molecules in both samples are oriented preferentially in the direction of the applied strain[25] (see, e.g., the spectra for sample A in Figure 3). The increased molecular orientation is seen in the higher ratio of the 1130/1060 cm$^{-1}$ Raman band areas, after cold-drawing, compared to the ratio observed for the undeformed material. For samples A and E this ratio is 25 and 13, respectively, after cold-drawing compared to a value of 1.8 for the undeformed materials A and E. Pigeon et al.[25] showed that this ratio rises with increasing molecular orientation for systems with uniaxial fiber symmetry. Cold-drawn sample A shows a larger orientational order than cold-drawn sample E. This may be related to the NDR of sample A which is larger than sample E (10.4 and 5.6, respectively).

**Effect of Polarization on Straining.** Raman spectra were taken from samples A and B during stepwise straining at 240 K. Initially, circular polarization ($^{\circlearrowright}I$) with no polarization analyzer was used (obtained with a $\lambda/4$ plate). Figure 4 shows the Raman spectra in the C−C stretching vibration region for sample A with

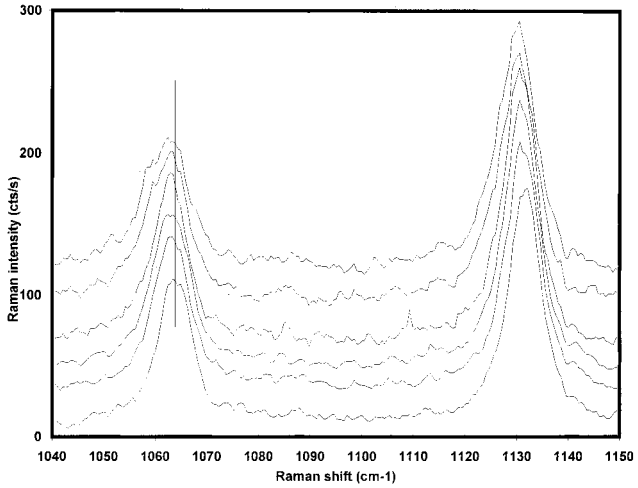


**Figure 4.** Spectra showing the C−C stretching Raman range recorded under $^{\circ}$I polarization conditions for cold-drawn sample A during stepwise straining experiments at 240 K and used to measure the band shifts for the 1060 and 1130 $cm^{-1}$ bands appearing in Figure 5. The 1295 $cm^{-1}$ Raman band is not shown. The spectra have been shifted in the Y direction for clarity. The spectrum at the bottom corresponds to the strainless situation.

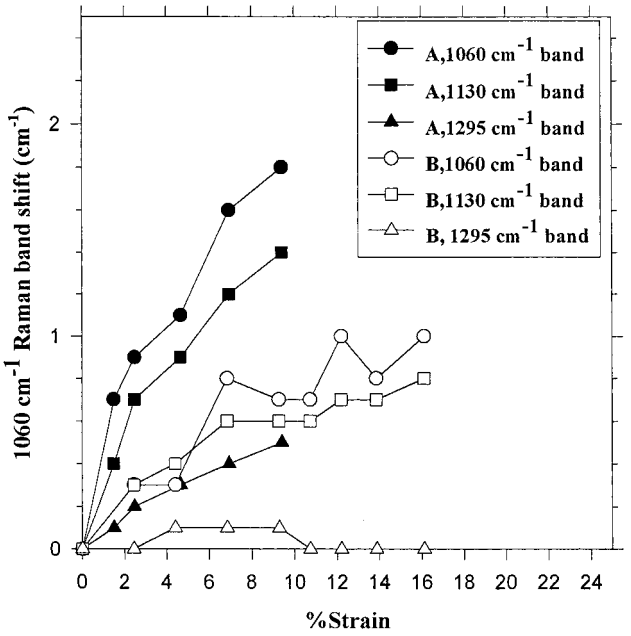


**Figure 5.** 1060, 1130, and 1295 $cm^{-1}$ Raman shifts at 240 K as a function of the percent of macroscopic strain measured under $^{\circ}$I polarization conditions for cold-drawn samples A (black symbols) and B (white symbols).

increasing strain. The bands shift gradually and some asymmetry develops at the highest strains. Figure 5 shows the 1060, 1130, and 1295 $cm^{-1}$ Raman bands as a function of the % strain for samples A and B. The C−C stretching vibrations (1060 and 1130 $cm^{-1}$) show the largest shifts and the $CH_2$ twisting the smallest. This is in agreement with previously reported results for ultradrawn PE fiber.[15,17−20] Sample A shows larger shifts per % strain for each band than sample B. These bands are originating from trans chain sequences.

A further experiment was performed with the laser light polarized parallel ($^{\parallel}$I) to the direction of straining and no polarization analyzer. In this geometry the molecules oriented parallel to the straining direction are preferentially examined. The calculated shifts for

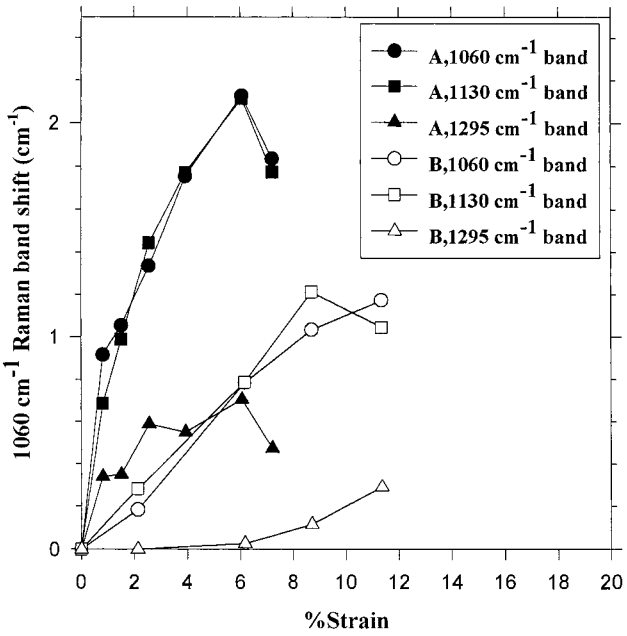


**Figure 6.** 1060, 1130, and 1295 $cm^{-1}$ Raman shifts at 240 K as a function of the percent of macroscopic strain measured under ($^{\parallel}$I) polarization conditions for cold-drawn samples A (black symbols) and B (white symbols).

samples A and B are shown in Figure 6. Sample A shows a large initial shift up to 1−2% macroscopic strain and subsequent increase of strain only results in a small further shift of the Raman band. Sample B, in contrast, shows a linear trend over the whole straining experiment. The 1060 $cm^{-1}$ initial band-shifts per % strain for sample A are 0.4 (up to 2%) and 0.65 for $^{\circ}$I and $^{\parallel}$I polarization, respectively. For sample B, these values are 0.09 and 0.12, respectively. The band shift is significantly larger for polarized light than for scrambled light.

The larger shift with parallel polarized excitation results from the polarized light preferentially exciting the molecules oriented parallel to the drawing direction, whereas circular polarization will in principle excite all of the molecules. The highest molecular stress is expected in the oriented molecules (i.e., parallel to the sample straining direction). Consequently, the band shifts per % strain are highest with parallel polarized laser light on the 1060 $cm^{-1}$ band. All the further experiments were carried out on this band and with parallel polarized laser light ($^{\parallel}$I).

**Band Shifts (Molecular Stress) per Unit Strain as a Function of Sample Characteristics.** Raman spectra were recorded during the uniaxial deformation at 240 K of samples A−G. The strain was increased stepwise to sample failure and the area analyzed remained fairly constant because the deformation was applied bidirectionally.

The 1060 $cm^{-1}$ band shift as a function of the macroscopic strain for samples A−G, with parallel polarization conditions ($^{\parallel}$I), are shown in Figure 7. The band position was determined by curve-fitting the 1060 $cm^{-1}$ band with a single band. The shift of the band toward the low wavenumber side occurs in all of the samples and is interpreted as a molecular strain in the all-trans C−C sequences. The material has been stretched to the natural draw ratio and further strain clearly loads the molecular chains rather than affecting the molecular orientation. Samples A and C and to

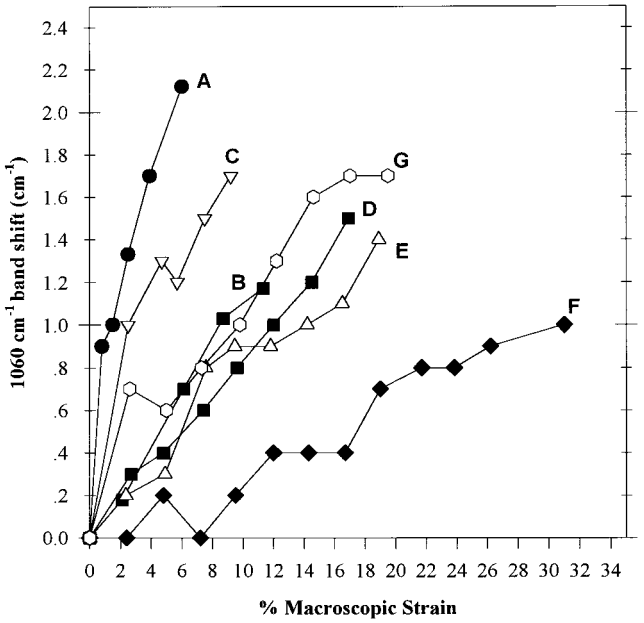


**Figure 7.** Shift of the 1060 $cm^{-1}$ Raman band under $^{\parallel}I_{\parallel}$ polarization conditions at 240 K as a function of the % strain for seven samples, i.e., for samples A−G. The 1060 $cm^{-1}$ Raman band for sample F has been corrected with the 1295 $cm^{-1}$ band position to make it reliable.

**Table 3. Rate of 1060 $cm^{-1}$ Band Shift per % Strain and Per True Stress for Samples A−G**

| samples | initial 1060 $cm^{-1}$ shift per % strain | initial 1060 $cm^{-1}$ shift per true stress ($cm^{-1}$/GPa) |
|---|---|---|
| A | 0.65 (up to 2% strain) | 4.4 (up to 2%) |
| B | 0.12 | 2.3 |
| C | 0.4 (up to 4% strain) | 4.1 (up to 4%) |
| D | 0.09 | 1.7 |
| E | 0.08 | 2.0 |
| F | 0.02 | 1.6 |
| G | 0.16 (up to 5% strain) | 2.2 (up to 5%) |

some extend G initially show a relatively high band shift during initial straining. The shift rate slows with further straining. For the other samples the shift is relatively linear with strain over the used strain levels.

The calculated band shift per macroscopic strain for each sample is shown in Table 3. Figure 8 shows these values plotted against the molecular weight ($M_w$). The calculations were performed using a least-squares straight lines fit through the data in Figure 7. Data from samples A, C, and G could not be satisfactorily fitted to a single line. For these samples we chose to fit with two lines, i.e., one for the first data points at low strain and another line for the data points at higher strain. For samples A, C, and G, the band shift per macroscopic strain was calculated on the basis of the tangent of the first line at low strain level. The fact that for samples A, C, and G the data points cannot be fitted to a single line suggests that at the measurement temperature, i.e., 240 K, still some sort of relaxation mechanism is active, which allows some relaxation at higher strain levels. We have to realize that for samples A, C, and G, the highest shifts are observed at low macroscopic strain, indicating a high molecular strain in these cases.

For the homopolymers A, B, and F the shift per strain decreases with increasing molecular weight (see Figure 8). Sample A, with the lowest molecular weight and ESCR, shows the largest band shift per strain. For sample F with the highest molecular weight and very

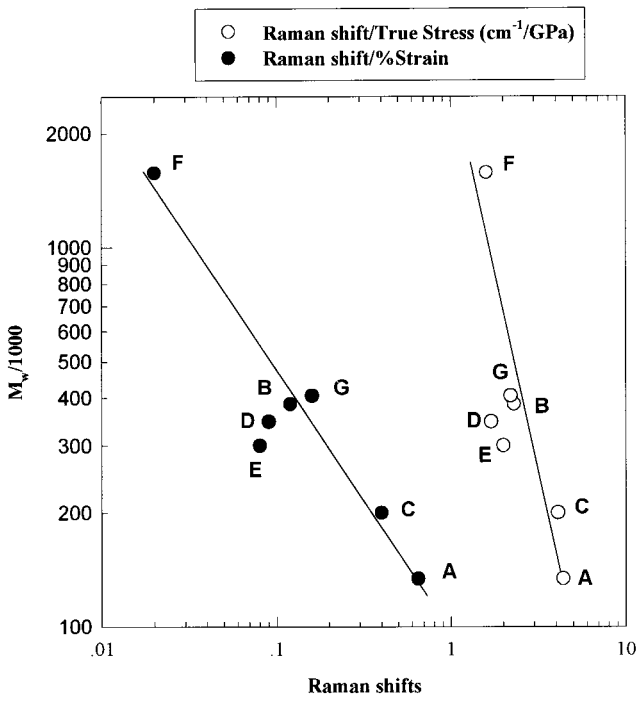


**Figure 8.** Plot on a log−log scale of the $M_w$ of the various samples versus the 1060 $cm^{-1}$ Raman band shifts per macroscopic strain and per true stress. Straight lines were drawn through the homopolymers A, B, and F.

high ESCR the lowest band shift per strain is observed. Additionally, sample A fails at the lowest % strain (in fibrillar bunches) and sample F at the highest % strain. Clearly, increasing molecular weight has the effect of reducing molecular stress per macroscopic strain and increasing the elongation at failure.

In addition to the effect of the molecular weight, also the effect of branching was studied. Sample C has a somewhat larger molecular weight than sample A and in addition 0.3 ethyl branches per 1000 C. The shift per strain is considerably lower for sample C than for sample A. Looking in Figure 8, the reduction of shift per % strain seen for sample C seems to fit in the molecular weight line (including the homopolymers A, B, and F). Therefore, the reduction in shift per % strain seems to be a molecular weight effect rather than a branching effect. This is in line with the general experience that branching of low molecular weight samples is not as effective in terms of material behavior as branching high molecular weight samples. For sample D the $M_w$ value is somewhat lower than that for sample B; however, sample D has ethyl branches (0.17 per 1000 C). In this case, the sample containing the branches (D) has a lower shift per % strain, which can be attributed to a branching effect. For sample E with 1.2 ethyl branches per 1000 C, the effect of chain branching is more clear. The shift per macroscopic strain is considerably lower than what is expected on the basis the $M_w$ of sample E. In conclusion, with the increasing number of ethyl branches the molecular strain per macroscopic stress is decreasing. However, the effect of branching is clearly smaller than the effect of molecular weight on the Raman shifts.

For sample G, having a relatively high $M_w$ and both ethyl and butyl branches, the shift per percent macroscopic strain is unexpectedly high. The latter is likely caused by its bimodal character anticipated by its very high polydispersity index ($M_w/M_n$). The shift of the 1060

$cm^{-1}$ Raman band per macroscopic strain resembles that of a rather high density material, like homopolymer sample B. This observation might shed some light on the discussion of the molecular architecture of these particular blended materials. It is known that the high density of this sample comes from the HDPE (high crystallinity) component of the blend and that the branched component will not effectively crystallize that much but induces tie molecules and other topological constraints. As the 1060 $cm^{-1}$ band is mainly sensitive to the all-trans fractions, which are in the crystals, the high-density side of the material is somewhat highlighted in the Raman experiments.

In relation to the ESCR behavior, it was observed that the samples with the lowest ESCR values (samples A and C) show the highest Raman band shift (i.e., higher molecular stress) for the same macroscopic strain. These samples show the highest densities. Additionally, the samples failed at lower molecular strains. These effects can be interpreted as resulting from an immediate loading of the crystalline phase with molecular strain. The cold-drawn structure is thought to be low-entangled since the tie molecules concentration is not expected to be extensive[9,26,27] (particularly for homopolymer A), and creep is expected to be rapid (Capaccio et al.[6]). Such a structure would be straightforward to pull out upon deformation, and further evidence is given by the high NDR of these samples. The crystals can slide along each other during deformation and failure occurs with breakage of the crystal structure. It was noted that both samples macroscopically failed in fibrillar bunches.

On the other hand, the samples with higher ESCR performance (samples B, D, E, and in particular F) showed a lower Raman shift (i.e., lower molecular stress) for the same macroscopic strain. Furthermore, the samples failed at higher absolute strains than the low ESCR materials. A different stress transfer to the molecular level can be anticipated for these samples. The molecular structure of the high ESCR materials is expected to be more complex and entangled than the low ESCR samples because the tie molecules are more likely to be present as the molecular weight and branch content increase (decreasing density)[9,26,27] and the structures of the initial cold-drawn materials are already more entangled since they show smaller NDRs and poorer molecular orientation (see copolymer E versus homopolymer A). Furthermore, a higher contribution of intercrystalline all-trans segments to the 1060 $cm^{-1}$ band is expected.

**Molecular Stress per True Stress.** The band shift per true stress ($cm^{-1}$/GPa) was calculated for the samples by using eq 1. The values are shown in Table 3 and plotted against $M_w$ in Figure 8.

$$\frac{\text{Initial "1060 cm}^{-1}\text{ band shift per \% strain"} \times 100}{\text{Initial modulus at 240 K}} \quad (1)$$

The band shift per stress ($cm^{-1}$/GPa), in particular for samples A and C (highest density samples), are close to those reported for the ultrahigh molecular weight polyethylene fibers, i.e., 5 $cm^{-1}$/GPa.[15] Furthermore, there appear to be fewer differences between the various samples as a consequence of correcting for the distinct *E*-moduli, achieved after cold-drawing. However, clearly the effect of molecular weight is still present; for samples A, B, C, and F (see the line in Figure 8). The effect of chain branching on the shift per stress is much lower (compare samples E and B [2.0 and 2.3]) (see Figure 8).

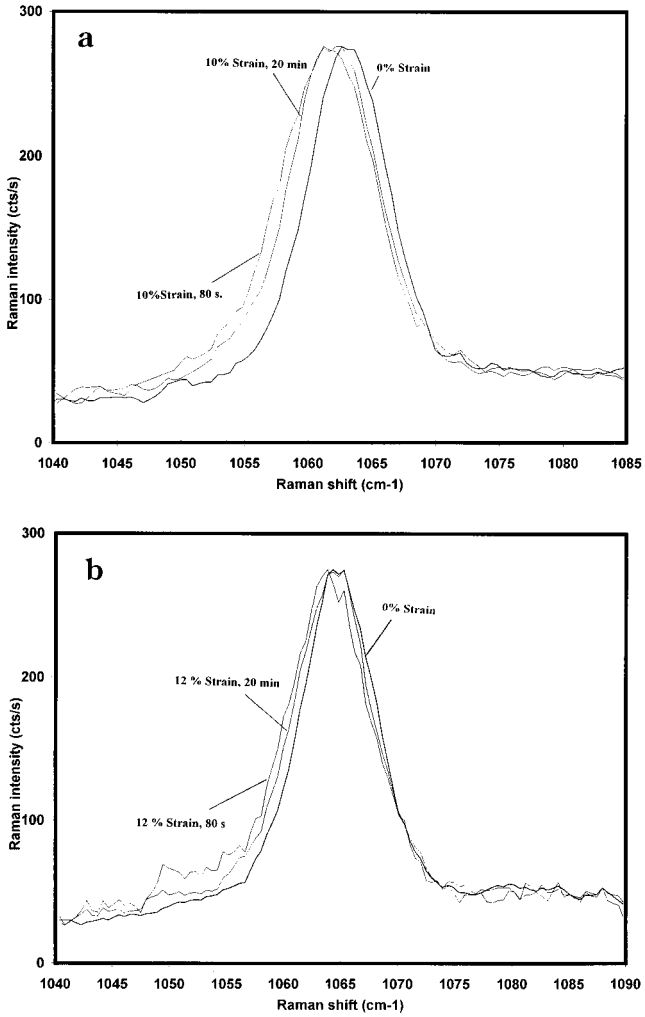


**Figure 9.** 1060 $cm^{-1}$ band at 240 K under $^{\|}$I polarization conditions at 0% strain, at 10% strain for sample B (a), and at 12% strain for sample E (b), and after 20 min keeping these stress levels.

**Molecular Relaxation at 240 K.** To examine the effects of relaxation at 240 K, further experiments were carried out where two cold-drawn polymers were stressed to a specific level. Subsequently, Raman spectra were accumulated as a function of time. Initially, sample B (homopolymer showing a molecular weight effect in Figure 8) was strained at 10% of strain, that is half of the strain at which this sample failed during the stepwise straining experiments. By comparing the *E*-moduli of the samples B and E, the percent of strain that should be applied to sample E (copolymer showing a branch effect in Figure 8) in order to achieve a similar stress level as for sample B can easily be calculated: 12% strain. For the experiments, samples B and E were strained up to 10% and 12%, respectively, and the stress relaxation was followed by taking Raman spectra sequentially. The Raman scans typically took 80−120 s using parallel ($^{\|}$I) polarization. In Figure 9a we show the asymmetrical C−C stretching band at 1060 $cm^{-1}$ for sample B recorded at 0%, recorded directly after applying 10% strain, and recorded 20 min after applying the 10% strain. For sample E, the results are shown in Figure 9b. In this case 12% strain was used. For sample B, clearly the shift of the 1060 $cm^{-1}$ band toward

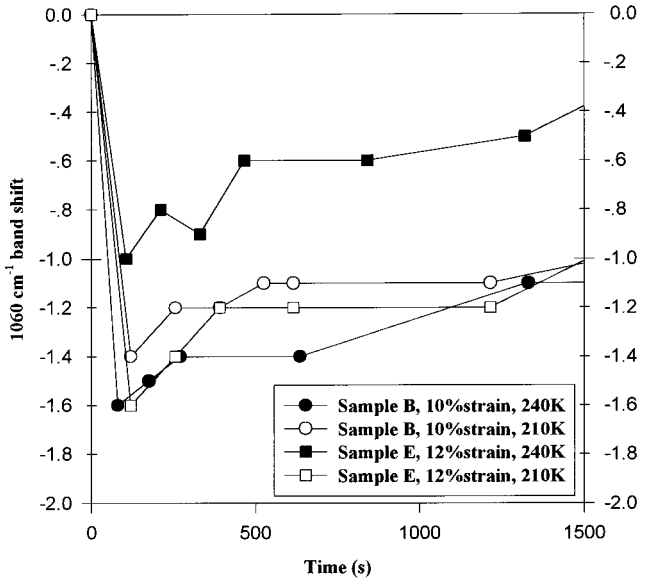


**Figure 10.** 1060 $cm^{-1}$ band shifts under ($^{II}$I) polarization conditions as a function of time for samples B (strained at 10%) and E (strained at 12% strain) at 240 K and at 210 K.

the low wavenumber side directly after applying the 10% strain is quite stable, the band is hardly shifted back after 20 min of relaxation. For sample E, the relative loss of the shift during the 20 min relaxation seems larger.

In addition, a stress relaxation experiment was carried out at a lower temperature (210 K) on homopolymer B and copolymer E to determine if stress relaxation occurs over a time scale comparable to the accumulation time of a spectrum. The same straining conditions as the 240 K experiments were used. The stress relaxation data for both samples at 210 and 240 K are shown in Figure 10. Copolymer E shows a larger initial shift at 210 K than at 240 K. This indicates that at 240 K this sample must be relaxing at a speed comparable to the accumulation time (120 s) of a single point and at 210 K this fast relaxation is slowed considerably. The relaxation behavior of homopolymer B appears to be virtually identical at 210 and 240 K.

## Conclusions

Raman spectroscopy was used to study molecular stress in a number of cold-drawn polyethylene grades. Raman data and ESCR test results were correlated. The samples with highest and lowest ESCR values were both shown to have a highly oriented molecular structure in the direction of the strain after cold-drawing. However, the low ESCR samples showed higher molecular orientation, in agreement with the higher NDR found with cold-drawing. Clearly, high molecular stress per macroscopic strain/stress on cold-drawn specimens can be correlated with low ESCR, whereas samples with higher ESCR performance showed a lower molecular stress per macroscopic strain/stress. The described behavior is related to the different molecular architecture of the materials, which transfers the macroscopic stress in different manners that can be well assessed under our experimental conditions.

Furthermore, a relation of the molecular stress per macroscopic strain/stress with the sample characteristics was observed. The results showed an important effect of molecular weight ($M_w$) on the molecular stress. The effect of chain branching on the molecular stress/macroscopic strain was found to be smaller. A bimodal copolymer showed a nontypical behavior with regard to the molecular stress as measured by Raman, which was related to its particular bimodal molecular design.

The large differences in ESCR between the homopolymer and the copolymers might be understood by comparing the molecular relaxation behavior of these materials. A copolymer did not show the same molecular stress as a homopolymer when strained to the same stress level, which implies that a higher molecular mobility (molecular relaxation) might occur in the latter sample. Further studies of molecular stress relaxation at elevated temperatures are now being performed, to fully characterize differences in molecular relaxation and the activation energies of this process and the relationship with macroscopic processes such as the α relaxation.

The Raman technique provides an alternative method of studying polyethylene grades in terms of ESC and material characteristics, requiring cold-drawn material and a quick rheo-optical test using Raman spectroscopy. Further experiments evaluating other grades need be undertaken in order to establish a quick and reliable ranking of materials and to gain a deeper understanding of the molecular processes involved in this type of failure.

**Acknowledgment.** We gratefully acknowledge BP Chemicals Grangemouth for supplying data on BSC and BTT. Dr. G. Struijk is thanked for experimental assistance and Dr. S. de Boer, Dr. R. Meier, and Dr. G. Capaccio are thanked for fruitful discussions. The management of DSM Research and of BP Chemicals are acknowledged for permission to publish this work.

## References and Notes

(1) Annual Book of ASTM Standards, Specification D 1693-70 (reapproved 1988).
(2) Cawood, M. J.; Sleeman, T. J. C. *Polym. Testing* **1980,** *142*, 191.
(3) Strebel, J. J. *Polym. Testing* **1995**, *14*, 189.
(4) Ward, A. L.; Lu, X. L.; Brown, N. *Polym. Eng. Sci.* **1990**, *30*, 1175. Ward, A. L.; Lu, X.; Huang, Y.; Brown, N. *Polymer* **1991,** *32*, 2172. Brown, N.; Lu, X.; Huang Y−L.; Qian, R. *Makromol. Chem., Macromol. Symp.* **1991**, *41*, 55.
(5) Cawood, M. J.; Channel, A. D.; Capaccio, G. *Polymer* **1993**, *34*, 423.
(6) Rose, L. J.; Channel, A. D.; Frey, C. J.; Gapaccio, G. *J. Appl. Polym. Sci.* **1994**, *54*, 2119.
(7) Lagarón, J. M.; Dixon, M.; Reed, W.; Pastor, J. M.; Kip, B. K. *Polymer*, in press.
(8) Lustiger, A.; Corneliusen, R. D. *J. Mater. Sci.* **1987**, *22*, 2470.
(9) Lustiger, A.; Ishikawa, N. *J. Polym. Sci., Polym. Phys.* **1991**, *29*, 1047.
(10) Brown, N.; Lu, X. *Polymer* **1995**, *36*, 453.
(11) Bower, D. I.; Maddams, W. F. *The Vibrational Spectroscopy of Polymers*; University Press: Cambridge, U.K., 1989.
(12) Siesler, H. W.; Holland-Moritz, K. *Infrared and Raman Spectroscopy of Polymers*; Marcel Dekker Inc.: New York, 1980.
(13) Wool, R. P.; Bretzlaff, R. S. *J. Polym. Sci.* **1986**, *B24*, 1039.
(14) Young, R. J.; Day, R. J. *Br. Polym. J.* **1989**, *21*, 17.
(15) Kip, B. J.; van Eijk, M. C. P.; Meier, R. J. *J. Polym. Sci.* **1991**, *B29*, 99.
(16) Galiotis, C.; Young, R. J.; Batchelder, D. N. *J. Polym. Sci., Polym. Phys. Ed.* **1983**, *21*, 2483.
(17) Prasad, K.; Grubb, D. T. *J. Polym. Sci.* **1989**, *B27*, 381.
(18) Prasad, K.; Grubb, D. T. *J. Polym. Sci.* **1990**, *B28*, 2199.
(19) van Eijk, M. C. P.; Leblans, P. J. R.; Meier, R. J.; Kip, B. J. *J. Mater. Sci. Lett.* **1990**, *9*, 1263.
(20) Moonen, J. A. H. M.; Roovers, W. A. C.; Meier, R. J.; Kip, B. J. *J. Polym. Sci.* **1992**, *B30*, 36.
(21) Schachtschneider, J. H.; Snyder, R. G. *Spectrochim. Acta* **1963**, *19*, 117.

(22) Strobl, G. R.; Hagedorn, W. *J. Polym. Sci., Polym. Phys. Ed.* **1978,** *16*, 1181.
(23) Failla, M. D.; Carella, J. M.; De Micheli, R. *J. Polym. Sci. Polym. Phys.* **1988**, *26*, 2433.
(24) Meier, R. J.; Kip, B. J. *Microbeam Anal.* **1994**, *3*, 61.
(25) Pigeon, M.; Prud'homme, R. E.; Pezolet, M. *Macromolecules* **1991**, *24*, 5687.
(26) Huang, Y.-L.; Brown, N. *J. Mater. Sci.* **1988**, *23*, 3648.
(27) Huang, Y.-L.; Brown, N. *J. Polym. Sci., Polym. Phys.* **1991**, *29*, 129.

MA9717606